

M. Y. Villeneuve · M. Ptito · C. Casanova

Global motion integration in the postero-medial part of the lateral suprasylvian cortex in the cat

Received: 2 August 2005 / Accepted: 1 January 2006
© Springer-Verlag 2006

Abstract In cats, the postero-medial part of lateral suprasylvian cortex (PMLS) is generally considered a key area for motion processing. While behavioral studies have indeed supported the role of PMLS cortex in higher order motion integration (Cereb Cortex 6:814–822, 1996), there is no evidence that individual PMLS cells can perform such analysis (Vis Neurosci 5:463–468, 1990; J Neurophysiol 63:1529–1543, 1990). Given the fundamental importance of understanding the neural substrate subtending higher order motion processing, we investigated whether PMLS neurons can signal the direction of motion of complex random dot kinematograms (RDKs) wherein comprising elements do not provide any local coherent motion cues. Results indicated that most PMLS cells (82%) can integrate the displacement of individual elements into a global motion percept. Their large receptive fields allowed the integration of motion for elements separated by large spatial intervals (up to 4°). In most cases, the analysis of complex RDK motion necessitated the contribution of the area of the visual field beyond the classical receptive field. None of the complex RDK-sensitive cells were found to be pattern-motion selective when tested with plaid patterns. Our results provide the first evidence that receptive fields of PMLS neurons can perform global motion analysis and support the behavioral evidence that this area is implicated in complex motion processing (Cereb Cortex 6:814–822, 1996). It also further corroborates the findings that PMLS neurons cannot signal the

true direction of a plaid pattern (Vis Neurosci 5:463–468, 1990; J Neurophysiol 63:1529–1543, 1990). Providing that these same neurons can signal the direction of complex RDKs, there may be distinct cortical mechanisms for processing different types of complex motion.

Keywords Complex motion · Higher order processing · Spatio-temporal integration · Extrastriate cortex

Introduction

In order to perceive the veridical direction of the motion of objects, local motion cues analyzed in primary visual areas must be integrated in higher order cortical areas (Rudolph and Pasternak 1996; Li et al. 2000, 2001; Brosseau-Lachaine et al. 2001; Castelo-Branco et al. 2002; Huk and Hegger 2002). In cats, it is generally considered that the regions constituting the lateral suprasylvian (LS) cortex are involved in higher order motion integration. This is especially true for the postero-medial part of the LS cortex (PMLS), which has been the most studied area of the suprasylvian region and is considered by some authors as the homologue of the middle temporal (MT) area of the primate brain (Spear 1991; Payne 1993; Dreher et al. 1996). Neurons in the PMLS cortex have large receptive fields that are, for the most part, exquisitely selective for the direction of motion along translational and frontal axes (Blakemore and Zumbroich 1987; Gizzi et al. 1990a, b; Minville and Casanova 1998; Li et al. 2000, 2001; Brosseau-Lachaine et al. 2001). Involvement of the PMLS cortex in motion processing has also been demonstrated behaviorally (Pasternak et al. 1989; Rudolph and Pasternak 1996; Sherk and Fowler 2002; Huxlin and Pasternak 2004). Very little is known about the capacity of PMLS neurons to combine local signals presented in their receptive fields into a coherent percept. More than a decade ago, Gizzi et al. (1990b) reported that PMLS neurons cannot signal the veridical motion of a plaid pattern, a stimulus

M. Y. Villeneuve · M. Ptito · C. Casanova (✉)
Laboratoire des Neurosciences de la Vision, École d'optométrie,
Université de Montréal, CP 6128, succ. Centre-ville,
Montréal, QC, Canada, H3C 3J7
E-mail: christian.casanova@umontreal.ca
URL: <http://www.mapageweb.umontreal.ca/casanovc>
Tel.: +1-514-3432407
Fax: +1-514-3432382

M. Y. Villeneuve
Département de Physiologie, faculté de Médecine,
Université de Montréal, Montréal, QC, Canada

used to demonstrate a neuron capacity to integrate local motion signals into a single coherent percept (Adelson and Movshon 1982). Subsequently, Li et al. (2001) presented evidence of pattern-motion selectivity in PMLS using a series of random-line stimuli, thus promoting the notion that PMLS is an early cortical stage of motion integration. To further examine the involvement of PMLS cortex in higher order motion processing, we investigated whether PMLS neurons can signal the global displacement of a “complex” random dot kinematogram (RDK) which necessitates the spatial and temporal integration of the dots displacement over an extended area of the visual field. This stimulus has been successfully used to study complex motion in the LP-pulvinar complex and the antero-medial part of the LS cortex (Dumbrava et al. 2001; Ouellette et al. 2004), both being reciprocally connected to PMLS. The coding of such complex pattern would indicate that the PMLS cortex is part of neuronal pathways subtending the higher level spatio-temporal integration necessary to detect the global displacement of objects in a complex visual scene.

Methods

Animal preparation

Adult cats of either sex weighing 2.5–4.5 kg were used in this study. All procedures were made in accordance with the guidelines of the Canadian Council for the Protection of Animals, and the experimental protocol was accepted by the ethics committee of the Université de Montréal. The cat was premedicated with a subcutaneous injection of acepromazine maleate (Atravet™ 1.0 mg/kg) and atropine (0.4 mg/ml; 0.1 ml/kg). Thirty minutes after the injection, anesthesia was induced by mask inhalation of 5% isoflurane (Forane®) mixed with O₂/N₂O (50:50) and gradually lowered and maintained at 2% for the initial surgery. The depth of anesthesia was determined by the lack of response to clamping the inter-digital web of the posterior paws. Oxygen blood saturation and heart rate were monitored using an oxygen saturation meter (Model 8500, Nonin Medical, Inc.).

Lidocaine hydrochloride (Xylocaine® 2%) was given at all points of incision or pressure points. Following cephalic vein cannulation and tracheotomy, muscular relaxation was obtained by injecting gallamine triethiodide (2%). The cat was then placed in a stereotaxic frame (D. Kopf). Throughout the experiment, the animal was artificially ventilated using a respiratory pump (Model 665, Harvard Apparatus) with an O₂/N₂O (33/66%) mixture supplemented with agent-specific Tec3-Ohmeda vaporizer of halothane (Fluothane®). Isoflurane was changed to halothane at the end of the surgical procedure to facilitate single-cell recordings as we have shown that halothane has a lesser depressive effect on cortical visual responsiveness than isoflurane (Villeneuve and Casanova 2003). End-tidal gas samples were drawn

from a non-rebreathing circuit through a tube positioned at a Y-piece connection at the oral end of the endotracheal tube. End-tidal CO₂ partial pressure was monitored by a capnometer (Normocap® 200, Datex-Ohmeda, Inc.) and kept constant between 28 and 38 mmHg by adjusting the rate and stroke volume of the respiratory pump. The core temperature was maintained at 37 ± 0.5°C by means of a feed back-controlled heating pad. Electroencephalogram (EEG) recordings were made with stainless steel screws of 2 mm diameter inserted in the frontal bone. Both EEG and electrocardiogram were monitored throughout the experiment (Axoscope, Axon Instruments, Inc., USA). The animals were continuously infused with 5% dextrose in lactated Ringer's injection solution containing gallamine triethiodide (50:50, 20 mg/kg/h). Pupils were dilated with atropine sulfate 1% (Isopto®) and nictitating membranes were retracted by local application of phenylephrine hydrochloride 2.5% (Mydfrin®). The eyes were protected using contact lenses of appropriate refractive power (plano or +2.00 diopters).

Craniotomies were performed at the posterior part of the suprasylvian sulcus of both hemispheres, at Horsley–Clarke coordinates AP 7 to –2 and ML 11 to 16, and the dura was incised to access the cortex. For a subgroup of five animals, control recordings were carried out in area 17. In these cases, craniotomies were made at coordinates AP –1 to –7 and ML 1 to 6.

Electrophysiological recordings

Single-unit activity recordings were performed using varnished tungsten microelectrodes (2–4 MΩ; A-M Systems, Inc.®) at a descending angle of ~40° and ~16° with respect to vertical for PMLS and area 17, respectively. The exposed cortex was covered with warm agar, over which melted wax was applied to create a sealed recording chamber. The signals were amplified, displayed on an oscilloscope and played through an audio monitor. Neuronal activity of the recorded units was isolated using a window discriminator (WPI) and fed to an acquisition program (spike2 v3.x, CED Cambridge, UK) via an analogue–digital interface (1401, CED). The responses were recorded as post-stimulus time histograms (PSTH) of 10 ms bin width.

Visual stimulation

Receptive fields were first mapped and characterized with the aid of a hand-held projector/ophthalmoscope and computer-generated stimuli. The eccentricity (azimuth and elevation with respect to the *area centralis*) of the receptive field center was measured. Each unit was then quantitatively tested using the visual stimulus software, Pixx 2.03 (Sentinel Medical Research Corp., QC, Canada) driven by a Macintosh G3 computer. The stimuli were back projected by an LCD projector

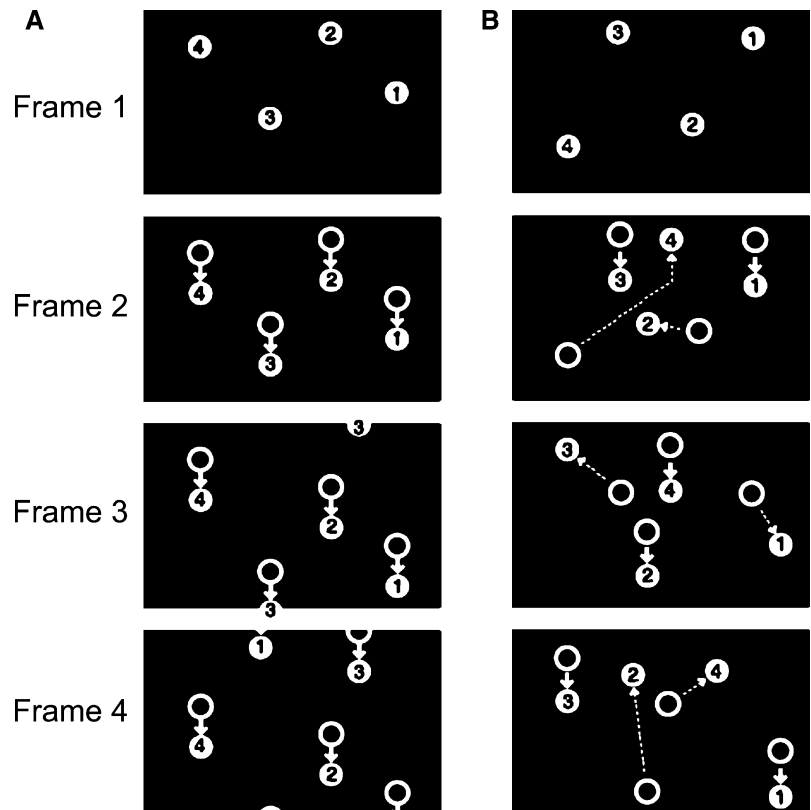
(InFocus Systems) onto a translucent screen placed 57 cm in front of the animal and subtending $70 \times 85^\circ$ of visual angle. The image had a resolution of 6.8 pixel/deg and the refresh rate was 67 Hz. The screen (Da-Lite) is made of a precise optical coating applied to an acrylic substrate (Da-Plex) allowing a high optical quality display and a uniform diffusion of the light projected onto it. Full-screen stimuli were presented for all cells. During each test, the activity for a blank screen of equal mean luminance (25 cd/m^2) was recorded (spontaneous activity level). Each stimulus presentation, as well as spontaneous activity recording, lasted 4 s and was repeated four times. Response levels were computed over the whole stimulus duration (4 s) and were expressed in spikes/second. Presentations were pseudo-randomly interleaved. Both eyes were stimulated when monocular stimulation was ineffective in driving a cell.

Sinusoidal drifting gratings (60% contrast) were first used to characterize the basic properties of PMLS neurons (e.g., orientation, spatial and temporal frequency selectivity).

Random dot kinematogram consisting of white circular dots on a black background (100% contrast) were used to study higher order motion processing. Optimization of the dot size was done in most cases along a range of 0.1° – 1° of visual angle. Due to the large receptive field of PMLS cells, the optimal responses were always obtained with 1° dots. Two stimuli were used to differentially emphasize global motion mechanisms. For convenience, these will be referred to as simple and

complex RDKs (Fig. 1). The simple RDK (panel a) was essentially a rigidly translating random dot field with no noise. In this configuration, each signal dot follows a straight and continuous path in one common direction. This stimulus required minimal simultaneous motion integration over an area of the visual field. For complex RDKs (panel b), the dots had a lifetime of two frames, i.e., they moved only once before being randomly repositioned, i.e., being displaced in another spatial location. Over a temporal sequence of a given set of displacements, 100% of the dots contributed to the global motion sequence. Each dot had an equal random probability of beginning at the first or second frame of their motion sequence. In that stimulus, half of the dots were displaced in the motion direction while the remaining half was repositioned randomly at a time. In other words, the signal and noise frames have been segmented by half on any given frame presentation so that when half of the dots give the motion signals the remaining ones repositioned themselves (the reverse being observed in the next sequence). This configuration is similar to the “*Combined* condition” described by Williams and Sekuler (1984) and to low motion test coherence of Newsome and Paré (1988). In the complex RDK, there is never more than a single *phi* motion jump before repositioning. Consequently, there must be spatial and temporal integration of the dots displacement over an extended area of the visual field in order to signal the veridical direction of the pattern, as previously shown in Dumbrava et al. (2001).

Fig. 1 Schematic representation of simple (a) and complex (b) RDKs. *Solid arrows* represents the motion signal. This signal follows a straight path in simple RDK. In complex RDK, *straight lines* represent motion signals while *broken lines* illustrate the random repositioning of the corresponding dot. Each *rectangle* represents one stimulus frame



Two main spatial parameters were investigated using complex RDKs: (1) the optimal spatial interval (D_{opt}), which corresponded to the distance between partner dots that provided the highest level of direction selectivity, and (2) the largest spatial interval (D_{max}), which corresponded to the largest interval at which direction selectivity was maintained. We also investigated the effect of varying the temporal interval (T) between the appearances of given partner dots, i.e., the duration of the single *phi* motion jump (computed between the extinction of the dot at its initial spatial position and the appearance of the dot at its new spatial location).

We also studied the effect of restricting the RDK pattern to the classical receptive field in 10 cells exhibiting clear boundaries. In those cases, the limits of the receptive fields of half of the cells that were initially assessed by hand were reassessed quantitatively using computer-controlled grating patches moving within and outside the previously defined area of activation. The grating was contained within a rectangular window ($70^\circ \times 2^\circ$ or $2^\circ \times 85^\circ$) that was randomly positioned along the vertical and horizontal axes of the receptive field (2° steps). For all cells tested, the area of activation was similar whether it was defined by hand or by computer-controlled stimuli. Direction selectivity to simple and complex RDKs was then evaluated as a function of stimulus size. On average, the area beyond the classical receptive field, which was stimulated by the full pattern, was around $5,600 \text{ deg}^2$ (from 5,312 to 5,840 deg^2).

For both simple and complex RDKs, direction selectivity was assessed by varying the direction of motion over 360° by incremental steps of 15° or 30° , and a direction index (DI) was computed as follows:

$$DI = 1 - \frac{\text{response in the non - preferred direction} - \text{spontaneous activity}}{\text{response in the preferred direction} - \text{spontaneous activity}}$$

A DI value of >0.5 indicates that the cell was selective for the direction of motion of the stimulus, whereas a DI of <0.5 indicates that the cell was not selective to the direction of motion (Minville and Casanova 1998). Criteria for determining the responsiveness of PMLS cells to the RDKs were as follows: first, the optimal response had to be at least twice the spontaneous discharge rate and be significantly different from the value of the SEM; secondly, cells were regarded as tuned for RDK direction when they responded to a specific range of directions (clear pattern of directional tuning). Consequently, their selectivity (optimal value) could be assessed quantitatively by measuring the bandwidth of tuning (quantified as half width measured at half height). In rare cases, the selectivity to complex RDKs was so broad that we could not compute a bandwidth with confidence.

For all direction-selective cells, responses to drifting plaid patterns were assessed. Plaids were composed of two superimposed identical sine wave drifting gratings differing in orientation by 120° . For each cell, the spatial

and temporal frequency of the comprising gratings corresponded to the optimal values computed from responses evoked by individual drifting gratings. The contrast of each plaid component was 30%. Responses to plaids were classified as pattern-motion (PM) selective or component-motion (CM) selective by calculating partial correlation coefficients using the following formula: $R_p = (r_p - r_c r_{pc}) / [(1 - r_c^2)(1 - r_{pc}^2)]^{1/2}$ (Movshon et al. 1986, corrected). R_p represents the partial correlation coefficient for the PM prediction, r_c the correlation coefficient of the plaid response and the CM prediction, r_p the correlation coefficient for the plaid response and the pattern prediction and r_{pc} the correlation coefficient for the two predictions. Similarly, R_c is the partial correlation coefficient defined for the CM prediction and is calculated by exchanging r_p with r_c in the equation. Component and pattern predictions were based on a neuron's direction tuning function to a drifting sine wave grating. The PM prediction is identical to the cell's actual response to the grating. To obtain the CM prediction, spontaneous activity is subtracted from the cell's response to the grating. The direction tuning function is then duplicated and each copy is shifted 60° in opposite directions. Both direction tuning functions and spontaneous activity are then summed.

Cells were tested either with 12 or 24 directions, thus influencing critical values (i.e., by changing the degrees of freedom). In order to present all data in one graph, partial correlation coefficients were transformed into Z scores (Majaj et al. 1999; Ouellette et al. 2004). Transformations to Z scores were performed with a modified (Sokal and Rohlf 1981) version of Fisher's transform:

$$Z_{R_p} = \frac{0.5 \ln \left(\frac{(1 + R_p)}{(1 - R_p)} \right)}{\sqrt{1/(n - 3)}}$$

Z_{R_c} can be calculated by replacing R_p with R_c . The n represents the number of directions at which the stimulus was presented. A cell was considered PM selective when the value of R_p (or Z_{R_p}) was significantly greater than R_c (or Z_{R_c}) and zero, as determined with a t test (one tail $\alpha = 0.05$). A CM-selective cell has an R_c (or Z_{R_c}) that is significantly greater than R_p (or Z_{R_p}) and zero (Smith et al. 2005).

Confidence intervals (π) were calculated to account for the variability that could occur in electrophysiological experiment. Since we cannot record all cells in a brain area, errors can be attributable to random sampling errors. Confidence intervals are made to confirm that the observed characteristics of our sample fall outside the random sampling errors and therefore are not attributable to chance. For each parameters tested, the confidence interval always fell outside the random

sampling error. Therefore, even with the relatively low number of cells tested, the results are stable enough to be generalized to all the cells in the area and are not attributable to chance.

Histology

Electrolytic lesions were made along recording tracks. At the end of each experiment, the animal was killed by an intravenous overdose of pentobarbital sodium (Euthanyl, 240 mg/ml, 2 cc/4.5 kg). The brain was removed from the skull and immersed in a solution of buffered formalin (10%). Forty-micrometer serial sections (coronal plane) were cut using a Microtome Cryostat HM500 OM (Microm International GmbH) and stained with cresyl violet. Verification of the position of the electrode tracks was made to confirm the location of recordings in PMLS and area 17.

Results

Response properties of 56 cells in the PMLS cortex and 21 cells in the primary visual cortex were investigated. The basic receptive field properties of PMLS cells recorded here were comparable to those described in earlier reports by others and us (Blakemore and Zumbroich 1987; Gizzi et al. 1990a, b; Guido et al. 1990; Minville and Casanova 1998; Li et al. 2000, 2001; Merabet et al. 2000; Brosseau-Lachaine et al. 2001). Recordings were made throughout the rostro-caudal extent of PMLS cortex and, consequently, receptive field eccentricities varied from 4° to 80°. Receptive fields were generally large and covered an area between 85 and 800 deg² (mean \pm SD 351.63 \pm 273.14 deg²; median of 240 deg²) and their size increased with eccentricity ($P < 0.001$). The mean optimal spatial frequency was 0.16 \pm 0.16 c/deg. Additionally, most PMLS cells (80%; 39/49 units) were direction selective to the drifting sine wave grating.

Direction selectivity to simple and complex RDKs

The vast majority of PMLS cells (35/41 cells; confidence intervals of percentages: 74.1% $< \pi <$ 96.7%) responded to simple RDK. The remaining cells were either poorly visually responsive and exhibited a high level of response variability or were lost before the completion of the tests. For all units, the optimal RDK parameters were determined by measuring responses as a function of dot density and speed. Examples of such simple RDK response curves are shown in Fig. 2. Panels a–c show the response profiles when dot density was varied. In general, PMLS neurons respond to dot densities lower than 0.09 dot/deg². The neurons exhibit band-pass (panel a; 48% of units) or low-pass (panel b; 36%) tuning functions. For a few cells, responses reached a plateau and optimal values were around 0.03–0.05 dot/deg² (panel c;

16%). Most neurons responded optimally to dot speed ranging between 10 and 50°/s, and a few preferred higher velocities (between 60 and 90°/s and some up to 120°/s). The median was 38.6°/s. Cells generally exhibited a clear band-pass tuning function as shown in panel d.

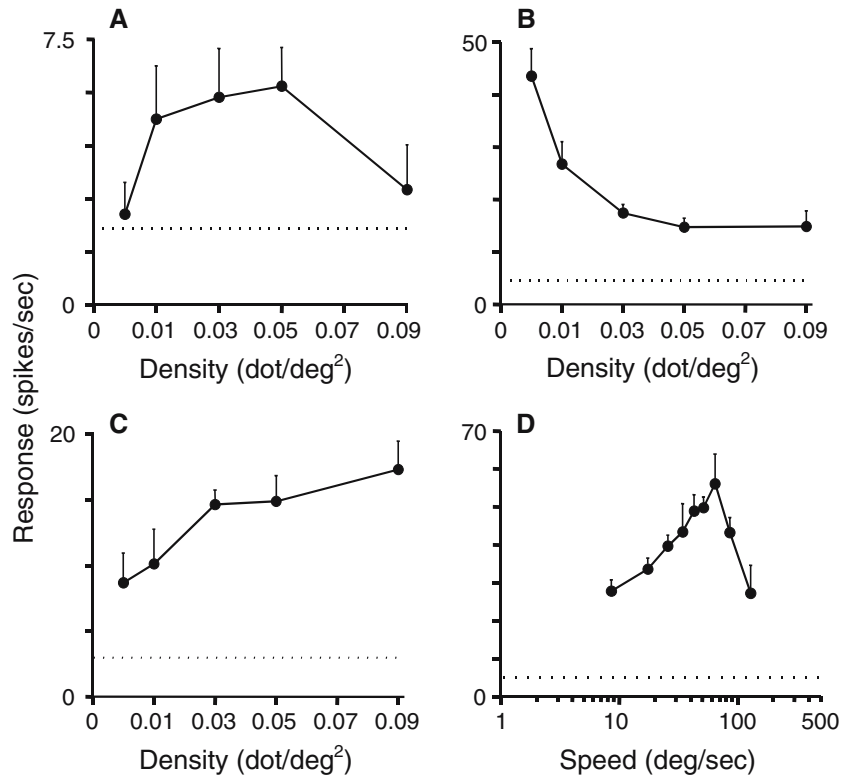
Almost all responsive PMLS neurons were direction selective (97%, 34/35 units; 91.1% $< \pi <$ 103%) for simple RDK. More interesting is the fact that 82% (27/33 units, one cell not tested for complex RDK; 67.7% $< \pi <$ 95.9%) of those direction-selective cells were also able to signal the direction of motion of complex RDKs. Three representative examples of simple and complex RDK-selective PMLS neurons are shown in Fig. 3 a–c. Panel a shows a unit exhibiting similar tuning functions and response strengths for both RDKs. The neuron depicted in panel b responded preferentially to the simple RDK. Panel c illustrates the fact that a subset of cells exhibited broader direction tuning functions for complex RDKs. Panel a of Fig. 4 presents the relationship between DI values computed with simple and complex RDKs. Most data points lie in the upper-right quadrant indicating that cells were direction selective for both stimuli. A closer examination of the graph shows that the vast majority of the data points are below the line of perfect regression, demonstrating that PMLS neurons are generally more strongly direction selective for simple than complex RDK (DIs of 0.94 \pm 0.11 and 0.72 \pm 0.25, respectively; $t = 5.05$, $P < 0.001$). At the extreme limit, three units were direction selective for simple RDK, but failed to signal the complex RDK direction (lower-right quadrant).

Panel b of Fig. 4 reveals that for nearly half of the cells tested, direction tuning functions computed from simple and complex RDKs were quite comparable (data points close to the line of perfect regression, see example in Fig. 3a). The other half behaved differently as they were more broadly tuned for complex than simple RDKs (data points located above the line; see example in Fig. 3c). This last observation stands when all cells are pooled together as mean direction bandwidths for simple and complex RDKs were, respectively, 52.6° \pm 20.3° and 70.9° \pm 27.7° ($t = 4.01$, $P = 0.001$).

Comparison between response strength (panel c) revealed that optimal discharges evoked by simple RDK were generally higher than the ones observed for complex RDK (mean of 21.79 \pm 13.77 and 15.13 \pm 12.36 sp/s, respectively, $t = 3.51$, $P = 0.002$; see example in Fig. 3b). The mean optimal velocity for simple (41 \pm 24.3 deg/s) was slightly less than that for complex motion RDKs (58.8 \pm 29.3 deg/s, $t = 2.29$, $P = 0.03$).

Therefore, most PMLS neurons can signal the direction of simple and complex motion-defined RDKs. A few neurons (six, 18%) could only signal the direction of simple RDKs. Mean receptive field size of complex RDK-selective cells was 332 deg² (distributed between 32 and 1,128 deg²), a value greater than that of cells which only responded to simple RDKs (ranged from 72 to 764 deg², mean of 295 deg²).

Fig. 2 Characterization of the responses evoked by simple RDKs: **a-c** show discharge rates of three PMLS cells as a function of dot density; **d** illustrates the response of a neuron to different RDK velocities. Error bars represent SEM. The dotted lines correspond to spontaneous activity levels



Comparison with responses to drifting gratings

Panel a of Fig. 5 presents the relationship between DIs computed for both types of RDKs and that computed from drifting gratings. Most data points are located in the upper-right quadrant (direction-selective cells), indicating that PMLS neurons remained direction selective for all three stimuli. A subset of cells lies in the upper-left quadrant, and these neurons were more direction selective for RDKs than for grating stimuli. Four direction-selective neurons for gratings did not showed strong direction selectivity for complex RDKs (lower-right quadrant). The mean DI computed from responses to drifting gratings was 0.73 ± 0.3 , a value significantly lower than those mentioned above for simple RDK ($t=4.1$, $P<0.0001$), but not significantly different from those of complex RDK ($t=0.61$, $P=0.544$).

Almost all PMLS cells exhibited broader direction tuning functions for simple and complex RDKs than for sine wave gratings. This is clearly illustrated in panel b of Fig. 5 which depicts the relationship between RDKs and grating bandwidths. Most data points are located above the perfect linear regression revealing that cells in PMLS are more broadly tuned for RDKs. The mean bandwidth for grating was $28^\circ \pm 12.3^\circ$, a value significantly different from that of simple ($t=8.78$, $P<0.001$) and complex RDKs ($t=8.61$, $P<0.001$; see values above).

Influence of the size of the RDKs

We investigated whether PMLS cells could discriminate the direction of RDK when the latter was restricted within the boundaries of their receptive field. Panels a and b of Fig. 6 present the responses of a PMLS cell to simple and complex RDKs, respectively. In both graphs, responses when the stimulus was either confined to the receptive field (empty symbols) or covering the full screen (filled symbols) are shown. Panel a illustrates the fact that changing the spatial extent of the simple RDK had little effect on direction selectivity. A clear preferred direction could be observed in full-screen condition ($DI=0.88$) as well as in the receptive field condition ($DI=0.88$). A different picture emerged when only the receptive field of the same neuron was stimulated with a complex RDK (panel b). The cell was direction selective in the full-screen condition ($DI=0.81$). However, the same unit failed to signal the direction of motion when the stimulus was restricted to its receptive field ($DI=0.32$) despite the fact that it exhibited a robust discharge rate. Panel d shows that the estimated proportion of direction-selective cells may vary according to the spatial extent of simple and complex RDKs. Overall, simple RDK direction-selective neurons remained direction selective irrespective of the stimulus size of the simple RDK (filled bars, $n=10$). However, for complex RDKs, the percentage of direction-selective cells was markedly reduced when the stimulus was restricted to

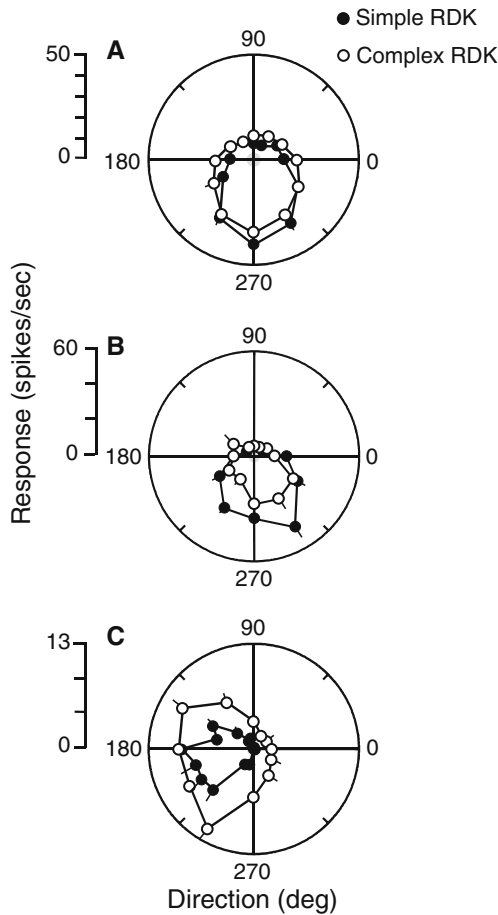


Fig. 3 Examples of responses \pm SEM to simple and complex RDKs: **a-c** show polar graphs illustrating the responses of three PMLS neurons to simple (*filled symbols*) and complex (*empty symbols*) RDKs drifted in 12 directions of motion. In **a-c**, DI for simple and complex RDKs are, respectively, 0.81 and 0.74; 0.89 and 0.79; 0.98 and 0.83. Bandwidths for simple and complex RDKs are, respectively, 62.3° and 82.5°; 66.3° and 77.8°; 44.5° and 76.3°

the cell receptive field (open bars, $n=9$), even though the moving pattern evoked robust discharges (the discharge rate was not significantly altered by the size of the stimulus; t test, $P=0.223$). Based on this subset of cells, PMLS neurons appeared to integrate information located beyond their classical receptive field in order to adequately signal the direction of motion of complex RDKs.

Influence of spatial and temporal intervals

The spatial interval between partner dots yielding optimal cell responses (D_{opt}) for complex RDK was determined for 29 cells. The D_{opt} was distributed between 0.57° and 2.85° of visual angle, with a mean of $1.91 \pm 0.72^\circ$. The largest spatial interval (D_{max}) for which a PMLS cell could still signal the direction of motion of a complex RDK ranged between 2.28° and 6.42° with a mean of $4.4 \pm 0.44^\circ$. An example is shown in panel a of Fig. 7. Varying the spatial interval between

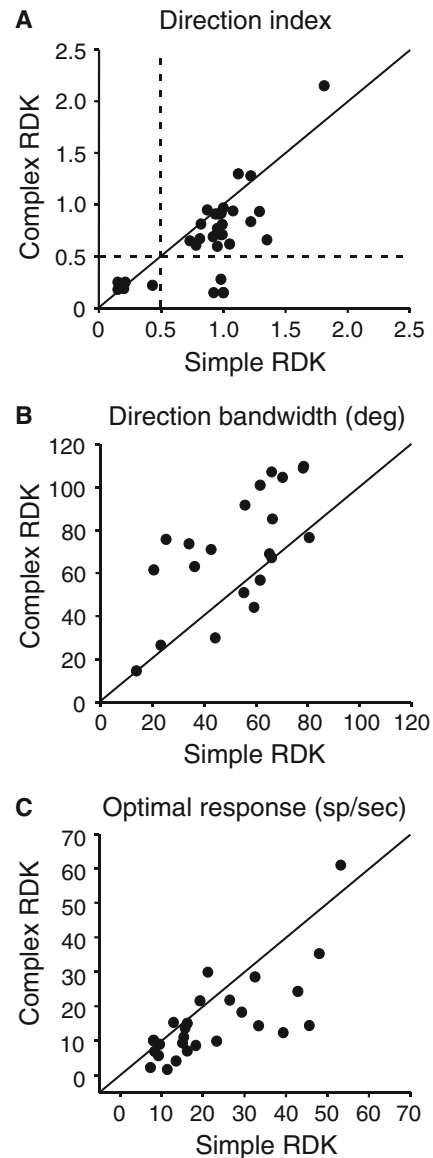


Fig. 4 Relationship between responses evoked by simple and complex RDKs. Direction indices (**a**), bandwidths (**b**), and optimal responses (**c**) were computed from RDKs tuning curves. In each graph, the line of perfect linear regression is shown. In **a**, the *dashed lines* represent the cut-off between directional and non-directional cells

the partner dots greatly influences the direction selectivity of the PMLS unit. The D_{opt} was at 1.14° (DI=0.86) and a further increase of the spatial interval yielded a decrease in response strength and direction selectivity. This cell was still able to code the direction of motion (DI=0.71) of the complex RDK for a spatial interval of 2.85° (D_{max}). D_{opt} and D_{max} values were investigated in relation to the receptive field size and no significant relationship could be determined (D_{opt} : $r=0.30$, $P=0.13$; D_{max} : $r=0.26$, $P=0.37$).

The responses of 14 cells were also studied as a function of the temporal interval (T) between the appearances of given partner dots, i.e., the duration of

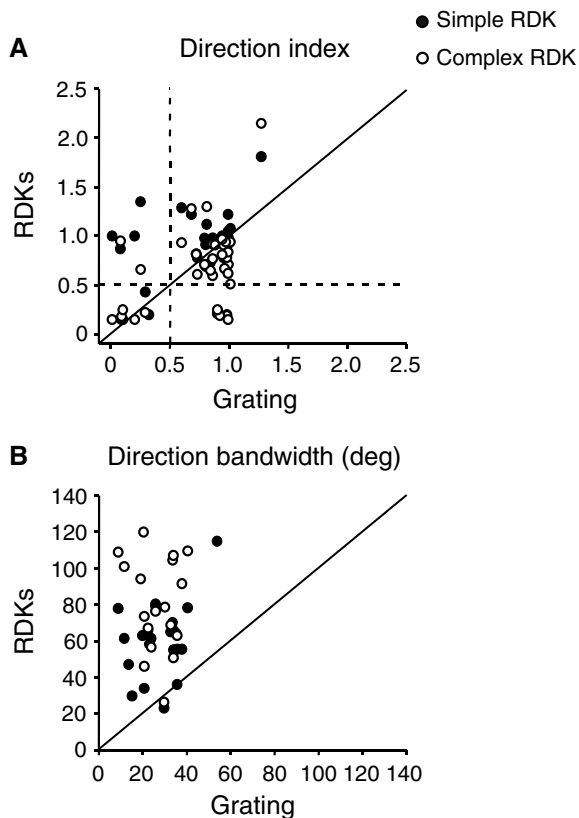


Fig. 5 Relationship between responses evoked by drifting sine wave gratings and simple (filled symbols) and complex RDKs (empty symbols): **a** direction index, **b** direction bandwidth

the single ϕ motion jump. All units behaved as the one shown in panel b of Fig. 7; i.e., optimal direction selectivity ($DI=0.86$ for this cell) was obtained for the shortest temporal interval (16 ms) technically possible. Direction selectivity and response strength were markedly reduced at T values greater than the optimal one.

Relationship with plaid pattern selectivity

When tested with plaid patterns, all complex RDK direction-selective cells were classified as component-motion selective, i.e., they only responded to the two components of the plaid. A representative example of such a cell is shown in Fig. 8. The cell tuning curve computed from plaid responses was bi-lobed (panel b) and did not match the pattern-motion prediction which would have corresponded to the tuning curve profile evoked by a single drifting grating (panel a). Despite its failure in signaling the true direction of motion of the plaid, the unit was direction selective for the complex RDK (panel c). The statistical analysis is illustrated in panel d and confirms the above observation, i.e., all data points computed from plaid responses of complex RDK direction-selective cells are located in the “component” area. Therefore there was

no relationship between complex RDK and pattern-motion selectivity in PMLS.

RDK responses of neurons in the primary visual cortex

For comparison purposes, we investigated the responsiveness of 21 neurons (8 simple and 13 complex) in area 17 to simple and complex RDKs (Fig. 9). Optimal RDK parameters were varied to evoke maximal discharge levels. All cells responded to the simple RDK, and 17 of those were direction selective. Almost all of these cells (15 out of 17) either could not be driven by the complex RDK (5 cells) or were not able to signal its direction of motion (15 cells), even if in most cases (9 cells), discharge levels were comparable to that observed with simple RDK. An example of the latter behavior is shown in panel a of Fig. 9. While the unit was direction selective to simple RDK ($DI=0.72$), it responded equally to all directions of motion of the complex RDK ($DI=0.24$). Panel b shows a similar phenomenon but in that case, responses to the complex RDK were weaker than that evoked by the simple RDK, when displaced in the preferred direction. Only two area 17 neurons (one complex and one simple cell) were found to be direction selective to complex RDK, i.e., a proportion (12%) much lower than that in PMLS (82%). These two cells did not present properties singularly different from the non-selective ones (RF of 48 and 14 deg^2).

Discussion

The present study demonstrates that PMLS neurons can signal the direction of a complex RDK which requires the integration of local motion over a large spatial area. Such processing cannot be fully performed by lower cortical areas, such as area 17, since the vast majority of cells in the primary visual cortex failed to signal the direction of motion for complex RDKs. This study also showed that PMLS cells have the capacity to bind local motion cues even if those cues are separated by relatively large spatial displacement. Moreover, we presented some evidence suggesting that the analysis of complex RDK motion necessitates the contribution of the area of the visual field beyond the classical receptive field.

Spatial and temporal integration

PMLS cells can integrate local motion cues even when the spatial displacement of each dot comprising the complex pattern is greater than 4° . It is of interest to note that in the context of the homology between cortical areas in cats and primates (e.g., Payne 1993), cells in the monkey area MT/V5 (Mikami et al. 1986) can integrate apparent motion with spatial intervals in a similar range as the PMLS cells studied here. We found no relationship between this level of spatial integration

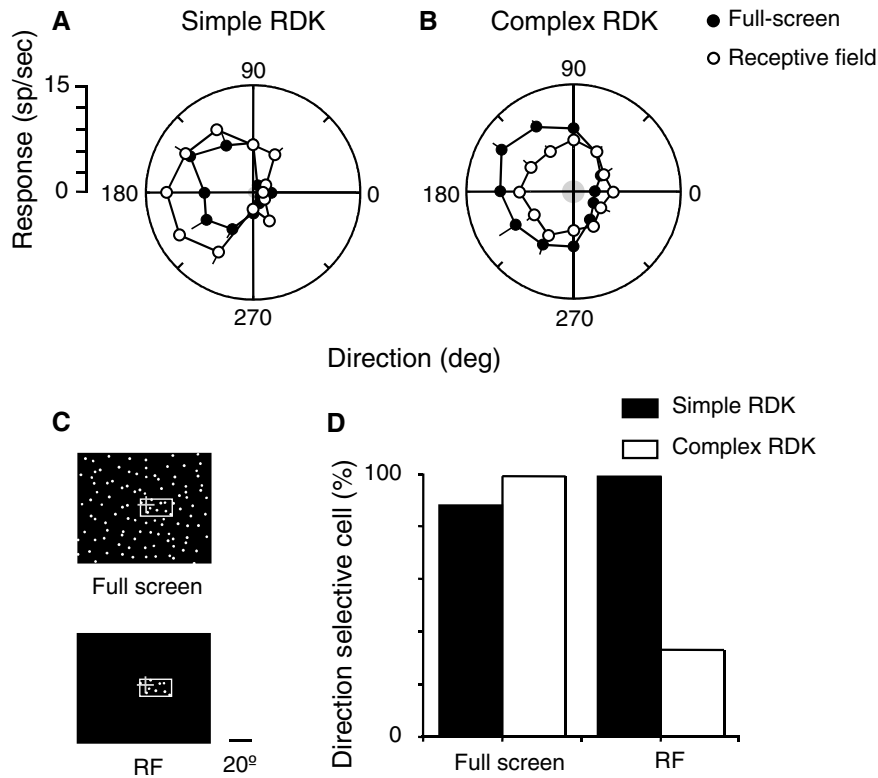


Fig. 6 Effects of restricting the RDK dimension to receptive field size. **a** and **b** show the responses of the same PMLS cell to full-screen stimulation and when the RDK is restricted to the receptive field size of the cell, for simple and complex RDKs, respectively. In **a**, the DI is 0.88 in both stimulus conditions, and the bandwidth is, respectively, 78.6° and 96° in full-field and receptive field conditions. In **b**, the cell responded selectively to complex RDK only to the full-screen RDK (DI of 0.84, bandwidth of 107°). Complex RDK could not trigger direction selectivity when

restricted to the size of the cell's receptive field (DI=0.33). *Error bars* represents SEM. *Shaded areas* in the polar graphs represent spontaneous activity levels. **c** shows the schematic representation of the receptive field of the PMLS cell in **a** and **b** in both conditions (full-screen and receptive-field-only stimulations). The *cross* represents the *area centralis*. **d** shows the percentage of direction-selective cells to simple (*filled bars*) and complex RDK (*empty bars*) as a function of the condition of stimuli presentation

(D_{max}) and the size of the receptive field of PMLS cells. Such a relationship was found in the LP-pulvinar complex (Dumbrava et al. 2001), a subcortical thalamic area interconnected with the PMLS cortex (Symonds et al. 1981; Updyke 1981; Tong et al. 1982; Raczowski and Rosenquist 1983; Abramson and Chalupa 1985; Norita et al. 1996). Receptive fields of neurons from the LP-pulvinar are on average larger than those from PMLS and were shown to code the direction of motion of complex RDK even when partner dots were spatially separated by more than 6.5° (Dumbrava et al. 2001). On the basis of its greater spatial integration capability, we can therefore propose that the LP-pulvinar can perform a higher order spatial integration based, in part, on signals from PMLS cells. This would support theoretical and experimental work (Mumford 1991; Singer 1994; Miller 1996; Sherman and Guillery 1996; Merabet et al. 1998) that proposes the involvement of thalamo-cortical loops (as computational networks) in the processing of complex information such as higher order motion signaling.

Our data also suggest that most PMLS cells can signal the direction of motion of complex RDKs only

when the latter stimulates the area beyond the classical receptive field. This would imply that the processing of complex motion in PMLS needs the involvement of other neurons. One possibility would be that neighboring neurons within the PMLS provide the necessary input to perform large-scale spatial integration, through intra-cortical connections (Downing and Movshon 1989; Brosseau-Lachaine et al. 2001). Cortical neurons outside the PMLS cortex may also contribute to this property, especially those in areas known to be involved in complex motion analysis (AMLS: Ouellette et al. 2004; PLLS: Li et al. 2000; DLS: Chen et al. 2004). A third possibility, which is not exclusive with the former ones, would be the contribution of afferents from subcortical nuclei involved in complex motion processing such as the LP-pulvinar complex (Dumbrava et al. 2001) which contains cells with receptive fields spatially encompassing those of PMLS neurons. In this case, it would further implicate cortico-thalamic loops in complex visual processing. Whatever the above assumptions are, these data suggest that the classical receptive field and surrounding ones act as a single integration unit.

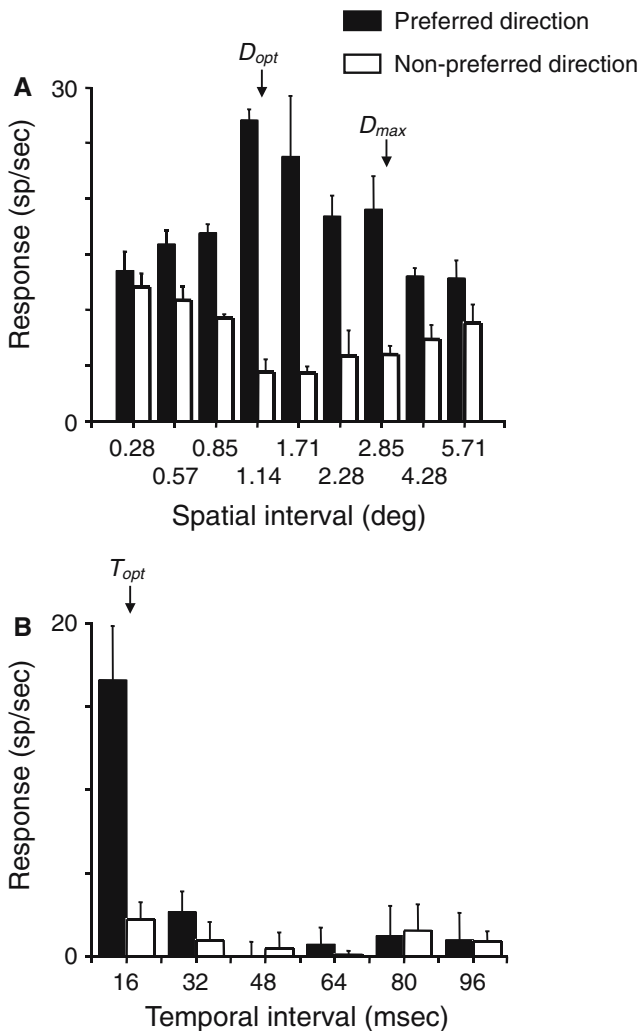


Fig. 7 Influence of spatial (a) and temporal interval (b) between partner dots on response strength and direction selectivity. In a, D_{opt} (1.14°) and D_{max} (2.85°), respectively, represent the optimal spatial interval for which the cell exhibits the strongest DI (0.86) and the largest spatial interval for which it remains direction selective (DI=0.71). In b, T_{opt} (16 ms) represents the optimal temporal interval for which the cell has the strongest direction selectivity (DI=0.86)

Mode of information processing in PMLS

Britten and Newsome (1998) and Heuer and Britten (2004) have provided evidence that the processing of direction of motion in areas MT and MST is more likely to be explained by a coarse rather than a sparse coding model, i.e., a given stimulus would excite a widely distributed population of MT/MST neurons [in a sparse model, neurons would be narrowly tuned and relatively few of them would be active at any moment (Barlow 1972; Lehky and Sejnowski 1990; Vinje and Gallant 2000, 2002)]. Our results support a coarse coding representation of stimulus direction in PMLS cortex, since most cells were direction selective and almost always broadly tuned for direction of motion, even for higher

order stimuli such as complex RDKs. In addition, our data showed that the coding mode in PMLS does not vary with stimulus context as appears to be the case in area V1 (Vinje and Gallant 2000 2002). In the present study, when compared to receptive field stimulation alone, full-screen stimulation did not change the discharge rate of PMLS cells [an augmentation or reduction of the discharge rate would have signified an increase in the coarseness or sparseness of the neural code, respectively (Vinje and Gallant 2000, 2002)]. However, the information transfer rate (Vinje and Gallant 2000, 2002) appears to decrease as most direction-selective PMLS neurons cannot code the direction of complex RDKs in receptive-field-only conditions even if they exhibit a discharge rate similar to that in full-screen conditions. In other words, for the same number of impulses, stimulation of the receptive field alone does not provide enough information to signal direction of motion.

Relevance to behavior

The observation that PMLS cells can signal the direction of motion of complex RDK is in agreement with the behavioral findings of Rudolph and Pasternak (1996). In the latter study, LS cortex lesions (which generally included the posterior part of the LS cortex, comprising the PMLS) resulted in severe behavioral deficits in the integration of local motion information. Rudolph and Pasternak (1996) acknowledged the fact that their findings could not be substantiated by the sole neurophysiological study that investigated complex motion sensitivity in PMLS, but with a stimulus fundamentally different in nature. Gizzi et al. (1990b) reported, indeed, that PMLS cells cannot signal the true direction of a plaid pattern (pattern-motion selectivity): an indication that PMLS cells do not have the capacity to bind local motion cues into a coherent percept. On the basis of these physiological data, Rudolph and Pasternak (1996) proposed that the effects of LS lesions were mediated through higher order motion areas such as the ectosylvian cortex [known to contain pattern-motion neurons (Scannell et al. 1996; Zabouri et al. 2003)] which would receive its essential motion inputs from the PMLS cortex. In the present study, we showed that PMLS cells have the capacity to integrate the displacement of partner dots comprising complex RDKs. Consequently, the behavioral motion deficits observed by Rudolph and Pasternak (1996) are most likely to result from the direct loss of PMLS neurons. Obviously, one has to be cautious in making such a statement because the RDKs used in both studies were different. In Rudolph and Pasternak's study, the RDK consisted of dots moving in offset directions within a range of 0°–360° (Pasternak et al. 1995). In the present study, the signal dots had the same direction of motion but were moved to a different spatial location after a single ϕ motion. Despite these differences, the two patterns are complex in nature as

Fig. 8 Relationship between plaid pattern and complex RDK direction selectivity of a single PMLS cell. Polar plots illustrating the direction tuning functions for **a** drifting grating, **b** plaid pattern, and **c** complex RDK are shown. *Shaded areas* represent spontaneous activity levels. **d** Scatter plot in which the partial correlation for pattern and component selectivity complex RDK-selective neurons are plotted against each other. The data space is divided into three statistical regions. All data points are falling in the lower right area, indicating that these cells were component-motion selective

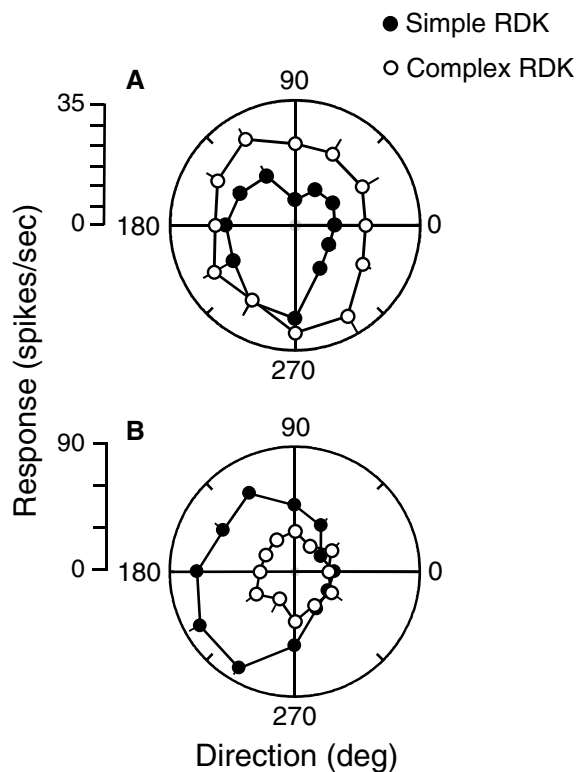
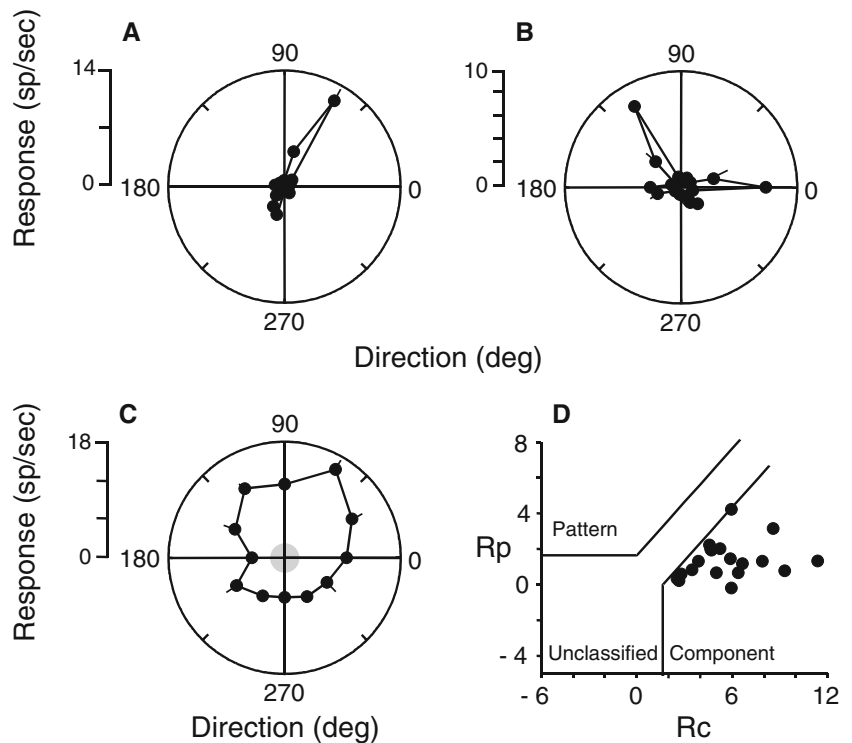


Fig. 9 RDK responses in area 17. **a** shows the responses to both RDKs of a simple cell (receptive field size of 20 deg²). This cell was direction selective for simple (DI of 0.72) but not for complex RDK (DI of 0.24). **b** illustrates the responses of a complex cell (receptive field size of 57 deg²). This cell was also direction selective for simple (DI of 0.73) but not for complex RDK (DI of 0.19). *Shaded areas* illustrate spontaneous activity levels

both necessitate the spatial integration of local directional signals into a global direction.

It is possible that other areas of the LS cortex may have contributed to the behavioral deficits. This is especially true for the antero-medial part of the LS cortex (AMLS) which contains both pattern-motion and complex RDK-selective neurons (Ouellette et al. 2004) and which is a direct target of PMLS neurons (Norita et al. 1996). The impact of the PLS cortex, the other main area that was also fully destroyed in Rudolph and Pasternak study, cannot be assessed because, to our knowledge, the complex motion sensitivity of its comprising neurons has not yet been investigated.

One may suggest that the conflicting results regarding pattern-motion in PMLS cortex may be related to the kind of anesthetic used (Pentobarbital sodium in Gizzi et al. 1990a, b; Urethane in Li et al. 2001; halothane in the present study) or to the anesthesia per se. Recent studies have indeed reported that the number of pattern-motion-selective units is greater in awake than in anesthetized animals (Pack et al. 2001; Guo et al. 2004). This affirmation has been refuted by Movshon et al. (2003) on methodological grounds (but see Pack et al. 2003). We do not believe that the absence of pattern-motion-selective units in the present study is due to anesthesia. In some animal preparations, we have recorded pattern-motion-selective neurons in the neighboring area, namely the AMLS cortex (Ouellette et al. 2004), the AEV cortex (Zabouri et al. 2003), and the LP-pulvinar complex (Merabet et al. 1998; Dumbrava et al. 2001).

Our study also confirmed the finding that PMLS cells are not pattern-motion selective (Gizzi et al. 1990b) and

consequently do not support the challenging findings of Li et al. (2001). These authors reported that a majority of PMLS cells were pattern-motion selective. However, they use a stimulus so fundamentally different (“random-line” pattern) that, in our opinion, it precludes any direct comparison between plaid-defined and random-line-defined pattern-motion. It is likely that the signaling of random-line patterns necessitates integration of its comprising small non-oriented elements over a larger spatial extent, similar to complex RDKs. Despite the absence of pattern-motion-selective units in PMLS cortex, on the other hand it may be possible that the comprising component-motion-selective neurons contribute to pattern-motion analysis by synchronizing their activity with similar cells in other areas such as area 18 (see Castelo-Branco et al. 2000). The fact that PMLS cells are direction selective to complex RDK but are not pattern-motion selective when tested with plaid patterns suggests the existence of two distinct or specialized mechanisms of motion integration at the cortical level, as we already proposed in the LP-pulvinar (Dumbrava et al. 2001). Although both types of stimuli require non-linear processing, only complex RDKs require long-range processing between neighboring cells in order to code for the direction of motion, while plaid patterns are more likely to be analyzed via rectification mechanisms (e.g., Wilson et al. 1992), without any necessary involvement of long-range interactions.

Acknowledgments This work was supported by a CIHR grant to C.C. We thank J.A. Movshon for information and formulas related to the novel method of analysis of plaid pattern responses. FRSQ provided most of C.C.’s salary (*Chercheur National* program). M.Y.V. was supported in part by a FRSQ—Vision Health Network Fellowship.

References

- Abramson BP, Chalupa LM (1985) The laminar distribution of cortical connections with the tecto- and cortico-recipient zones in the cat’s lateral posterior nucleus. *Neuroscience* 15:81–95
- Adelson EH, Movshon JA (1982) Phenomenal coherence of moving visual patterns. *Nature* 300:523–525
- Barlow HB (1972) Single units and sensation: a neuron doctrine for perceptual psychology? *Perception* 1:371–394
- Blakemore C, Zumbroich TJ (1987) Stimulus selectivity and functional organization in the lateral suprasylvian visual cortex of the cat. *J Physiol (Lond)* 389:569–603
- Britten KH, Newsome WT (1998) Tuning bandwidths for near-threshold stimuli in area MT. *J Neurophysiol* 80:762–770
- Brosseau-Lachaine O, Faubert J, Casanova C (2001) Functional sub-regions for optic flow processing in the posteromedial lateral suprasylvian cortex of the cat. *Cereb Cortex* 11:989–1001
- Castelo-Branco M, Goebel R, Neuenschwander S, Singer W (2000) Neural synchrony correlates with surface segregation rules. *Nature* 405:685–689
- Castelo-Branco M, Formisano E, Backes W, Zanella F, Neuenschwander S, Singer W, Goebel R (2002) Activity patterns in human motion-sensitive areas depend on the interpretation of global motion. *Proc Natl Acad Sci USA* 99:13914–13919
- Chen H, Li B, Diao YC (2004) Response properties of neurons in cat dorsal lateral suprasylvian cortex to optic flow fields. *Neuroreport* 15:1019–1023
- Downing CJ, Movshon JA (1989) Spatial and temporal summation in the detection of motion in stochastic random dot display. *Invest Ophthalmol Vis Sci Suppl* 30:72
- Dreher B, Djavadian RL, Turlejski KJ, Wang C (1996) Areas PMLS and 21a of cat visual cortex are not only functionally but also hodologically distinct. *Prog Brain Res* 112:251–276
- Dumbrava D, Faubert J, Casanova C (2001) Global motion integration in the cat’s lateral posterior-pulvinar complex. *Eur J Neurosci* 13:2218–2226
- Gizzi MS, Katz E, Movshon JA (1990a) Spatial and temporal analysis by neurons in the representation of the central visual field in the cat’s lateral suprasylvian visual cortex. *Vis Neurosci* 5:463–468
- Gizzi MS, Katz E, Schumer RA, Movshon JA (1990b) Selectivity for orientation and direction of motion of single neurons in cat striate and extrastriate visual cortex. *J Neurophysiol* 63:1529–1543
- Guido W, Tong L, Spear PD (1990) Afferent bases of spatial- and temporal-frequency processing by neurons in the cat’s posteromedial lateral suprasylvian cortex: effects of removing areas 17, 18, and 19. *J Neurophysiol* 64:1636–1651
- Guo K, Benson PJ, Blakemore C (2004) Pattern motion is present in V1 of awake but not anaesthetized monkeys. *Eur J Neurosci* 19:1055–1066
- Heuer HW, Britten KH (2004) Optic flow signals in extrastriate area MST: comparison of perceptual and neuronal sensitivity. *J Neurophysiol* 91:1314–1326
- Huk AC, Heeger DJ (2002) Pattern-motion responses in human visual cortex. *Nat Neurosci* 5:72–75
- Huxlin KR, Pasternak T (2004) Training-induced recovery of visual motion perception after extrastriate cortical damage in the adult cat. *Cereb Cortex* 14:81–90
- Lehky SR, Sejnowski TJ (1990) Neural model of stereoacuity and depth interpolation based on a distributed representation of stereo disparity. *J Neurosci* 10:2281–2299
- Li B, Li BW, Chen Y, Wang LH, Diao YC (2000) Response properties of PMLS and PLLS neurons to stimulated optic flow patterns. *Eur J Neurosci* 12:1534–1544
- Li B, Chen Y, Li BW, Wang LH, Diao YC (2001) Pattern and component motion selectivity in cortical area PMLS of the cat. *Eur J Neurosci* 14:690–700
- Majaj N, Carandini M, Smith MA, Movshon JA (1999) Local integration of features for the computation of pattern direction by neurons in macaque area MT. *Soc Neurosci Abstr* 25:674
- Merabet L, Desautels A, Minville K, Casanova C (1998) Motion integration in a thalamic visual nucleus. *Nature* 396:265–268
- Merabet L, Minville K, Ptitto M, Casanova C (2000) Responses of neurons in the cat posteromedial lateral suprasylvian cortex to moving texture patterns. *Neuroscience* 97: 611–623
- Mikami A, Newsome WT, Wurtz RH (1986) Motion selectivity in macaque visual cortex. II. Spatiotemporal range of directional interactions in MT and V1. *J Neurophysiol* 55:1328–1339
- Miller R (1996) Cortico-thalamic interplay and the security of operation of neural assemblies and the temporal chains in the cerebral cortex. *Biol Cybern* 75:263–275
- Minville K, Casanova C (1998) Spatial frequency processing in the posteromedial lateral suprasylvian cortex does not depend on the projections from the striate-recipient zone of the cat’s lateral posterior-pulvinar complex. *Neurosciences* 84:699–711
- Movshon JA, Adelson EH, Gizzi MS, Newsome WT (1986) The analysis of moving visual patterns. In: Chagas C, Gattass R, Gross C (eds) *Pattern recognition mechanisms*. Springer, Berlin Heidelberg New York, pp 148–164
- Movshon JA, Albright TD, Stoner GR, Majaj NJ, Smith MA (2003) Cortical responses to visual motion in alert and anesthetized monkeys. *Nat Neurosci* 6:3
- Mumford D (1991) On the computational architecture of the neocortex. I. The role of the thalamo-cortical loop. *Biol Cybern* 65:135–145
- Newsome WT, Paré EB (1988) A selective impairment of motion perception following lesions of the middle temporal visual area (MT). *J Neurosci* 8:2201–2211

- Norita M, Kase M, Hoshino K, Meguro R, Funaki S, Hirano S, McHaffie JG (1996) Extrinsic and intrinsic connections of the cat's lateral suprasylvian visual area. *Prog Brain Res* 112:231–250
- Ouellette BG, Minville K, Faubert J, Casanova C (2004) Simple and complex visual motion response properties in the anterior medial bank of the lateral suprasylvian cortex. *Neuroscience* 123:231–245
- Pack CC, Berezovskii VK, Born RT (2001) Dynamic properties of neurons in cortical area MT in alert and anaesthetized macaque monkeys. *Nature* 414:905–908
- Pack CC, Berezovskii VK, Born RT (2003) Reply to 'Cortical responses to visual motion in alert and anesthetized monkeys'. *Nat Neurosci* 6:3–4
- Pasternak T, Horn KM, Maunsell JH (1989) Deficits in speed discrimination following lesions of the lateral suprasylvian cortex in the cat. *Vis Neurosci* 3:365–375
- Pasternak T, Tompkins J, Olson CR (1995) The role of striate cortex in visual function of the cat. *J Neurosci* 15:1940–1950
- Payne BR (1993) Evidence for visual cortical area homologs in cat and macaque monkey. *Cereb Cortex* 3:1–25
- Raczkowski D, Rosenquist AC (1983) Connections of the multiple visual cortical areas with the lateral posterior-pulvinar complex and adjacent thalamic nuclei in the cat. *J Neurosci* 3:1912–1942
- Rudolph KK, Pasternak T (1996) Lesions in cat lateral suprasylvian cortex affect the perception of complex motion. *Cereb Cortex* 6:814–822
- Scannell JW, Sengpiel F, Tovee MJ, Benson PJ, Blakemore C, Young MP (1996) Visual motion processing in the anterior ectosylvian sulcus of the cat. *J Neurophysiol* 76:895–907
- Sherk H, Fowler GA (2002) Lesions of extrastriate cortex and consequences for visual guidance during locomotion. *Exp Brain Res* 144:159–171
- Sherman SM, Guillery RW (1996) Functional organization of thalamocortical relays. *J Neurophysiol* 76:1367–1395
- Singer W (1994) Neurobiology. A new job for the thalamus. *Nature* 369(6480):444–445
- Smith MA, Maja NJ, Movshon JA (2005) Dynamics of motion signaling by neurons in macaque area MT. *Nat Neurosci* 8:220–228
- Sokal RR, Rohlf FJ (1981) *Biometry*, 2nd edn. W.H. Freeman, New York, pp 561–690
- Spear PD (1991) Functions of extrastriate visual cortex in non-primate species. In: Leventhal AG (ed) *The neural basis of visual function*. Macmillan Press, London, pp 339–370
- Symonds LL, Rosenquist AC, Edwards SB, Palmer LA (1981) Projections of the pulvinar-lateral posterior complex to visual cortical areas in the cat. *Neuroscience* 6:1995–2020
- Tong L, Kalil RE, Spear PD (1982) Thalamic projections to visual areas of the middle suprasylvian sulcus in the cat. *J Comp Neurol* 212:103–117
- Updyke BV (1981) Projections from visual areas of the middle suprasylvian sulcus onto the lateral posterior complex and adjacent thalamic nuclei. *J Comp Neurol* 201:477–506
- Villeneuve MY, Casanova C (2001) Complex motion integration in the cat PMLS cortex. *SFN Abstr* 27:165.1
- Villeneuve MY, Casanova C (2003) On the use of isoflurane versus halothane in the study of visual response properties of single cells in the primary visual cortex. *J Neurosci Methods* 129:19–31
- Vinje WE, Gallant JL (2000) Sparse coding and decorrelation in primary visual cortex during natural vision. *Science* 287:1273–1276
- Vinje WE, Gallant JL (2002) Natural stimulation of the nonclassical receptive field increases information transmission efficiency in V1. *J Neurosci* 22:2904–2915
- Williams DW, Sekuler R (1984) Coherent global motion percepts from stochastic local motions. *Vision Res* 24:55–62
- Wilson HR, Ferrera V, Yo C (1992) A psychophysically motivated model for two-dimensional motion perception. *Vis Neurosci* 9:79–97
- Zabouri N, Ptito M, Casanova C (2003) Complex motion sensitivity of neurons in the visual part of the anterior ectosylvian cortex. *SFN Abstr* 29:179.4